Title

Steady-State and Transient Radionuclide Transport Through Penetrations in Nuclear Waste Containers

Authors

Chambre, P.L.
Lee, W.W.-L.
Kim, C.L.
et al.

Publication Date

1986-07-01

Lawrence Berkeley Laboratory
UNIVERSITY OF CALIFORNIA

EARTH SCIENCES DIVISION

STEADY-STATE AND TRANSIENT RADIONUCLIDE TRANSPORT THROUGH PENETRATIONS IN NUCLEAR WASTE CONTAINERS

P.L. Chambré, W.W-L. Lee, C.L. Kim, and
T.H. Pigford

July 1986

Prepared for the U.S. Department of Energy under Contract DE-AC03-76SF00098

DISCLAIMER

LBL-21806
UCB-NE-4084
UC-70

STEADY-STATE AND TRANSIENT RADIONUCLIDE TRANSPORT THROUGH PENETRATIONS IN NUCLEAR WASTE CONTAINERS

P. L. Chambre', W. W.-L. Lee, C. L. Kim and T. H. Pigford

Earth Sciences Division, Lawrence Berkeley Laboratory

and

Department of Nuclear Engineering, University of California

Berkeley, CA 94720

July 1986

Prepared for the U. S. Department of Energy under contract
DE-AC03-76SF00098

CONTENTS

1. Introduction 1

2. Radionuclide Transport Through an Aperture in a Waste Form Container 4

2.1 The Model Equations 4
2.2 The Transient Mass Flux 7
2.3 The Steady-State Mass Flux 10

3. Numerical Illustrations 20

3.1 Radionuclide Diffusion from a Single Hole 20
3.2 Diffusion-Controlled Mass Release Rate Through a Hole 22
3.3 Multiple Apertures on the Surface of a Cylindrical Waste Form 23
3.4 Release Rate from Multiple Apertures in a Container in Contact with a Porous Medium 24
3.5 Effect of a Water Gap Between Container and Porous Medium 27

4. Conclusions 33

5. Nomenclature 35

6. References 37

LIST OF FIGURES

Figure 1a The Coordinate System

Figure 1b Aperture Shapes

Figure 1c Bounding Contours

Figure 2 The Time-Dependent Shape Factor

Figure 3 The Steady-State Shape Factor Ratio (Epllipse/Circle) as a Function of Semi-Axis Ratio

Figure 4 The Magnitude of the Local Flux Function $g_1(M,O)$ for a Circular Aperture

Figure 5 Analogue Circuit and Steady-State Shape Factor for a Wall of Finite Thickness

Figure 6 Surfaces of Non-dimensional Concentrations and Diffusional Paths Near an Aperture

Figure 7 Radionuclide Transfer Rates From Multiple Holes and a Bare Waste Cylinder

Figure 8 Geometry for a Water Gap Between Container and Porous Rock

Figure 9 Radionuclide Transfer Rates from Multiple Holes Facing a Water Gap and from a Bare Waste Cylinder

1. Introduction

In this report we analyze the transport of radionuclides through penetrations in waste containers. Penetrations may result from corrosion or cracks and may occur in the original container material, in degraded or corroded material, or in deposits of corrosion products. In this report we do not consider how these penetrations occur or the characteristics of expected penetrations in waste containers. We are concerned here only with the analytical formulation and solutions of equations to predict rates of mass transfer through penetrations of specified size and geometry. Expressions for the diffusive mass transfer rates through apertures are presented in Chapter 2, and numerical illustrations are presented in Chapter 3. The calculations show that mass transfer through small penetrations in thin-wall containers can be great enough that the penetrated container is no longer an effective barrier for radionuclide release. Use of this theory to calculate mass transfer through thick-wall containers is the subject of a later report.

Studying mass transfer through container penetrations is relevant to demonstrating compliance with the U. S. Nuclear Regulatory Commission's performance objectives[1] for the waste-package subsystem that call for substantially complete containment within the waste package for 300 to 1000 years and require that the release rate of any radionuclide from the

engineered-barrier system following the containment period shall not exceed one part in 100,000 per year of the inventory of that radionuclide calculated to be present at 1,000 years. These studies also help define the extent to which Zircaloy cladding of spent-fuel waste can be relied upon as a barrier, and they contribute to a more detailed and mechanistic analysis of mass transfer from waste packages. Our previous analyses[2] of waste dissolution rate have considered only the simplified system of a bare waste form, with no container, surrounded by porous backfill and rock.

Chapter 2 presents the derivation of the time-dependent radionuclide diffusion through a hole of arbitrary geometry. Dependence of mass-transfer rate on hole shape is illustrated for elliptical and circular holes. Use of the equations to obtain bounding values for irregularly shaped holes is illustrated. The influence of hole shape on mass transfer varies with time, a result important in designing experiments to verify these predictions. Also provided are early-time and large-time approximations for calculating mass-transfer rate, as well as steady-state analyses of the concentration field and local concentration gradients in the vicinity of a circular hole.

Chapter 3 presents numerical illustrations for steady-state mass-transfer rates through a circular hole, including concentration isopleths. The results are extended to multiple holes, including a criterion for hole spacing wherein

superposition of single-hole solutions can be used. It is shown that numerous small holes in a thin-wall container can increase the mass transfer above that of a waste form not enclosed in a container.

These results point to the importance of considering small holes and cracks in evaluating the effectiveness of a container or fuel cladding as a barrier. Spent fuel cladding can be expected to have small perforations from manufacturing defects and the reactor environment. Additional perforations can be expected during pre-emplacement storage, handling, and exposure to the repository environment.

In Chapter 3 we also present a simplified analysis of multiple holes facing a water gap. If diffusion is the only transport mechanism, then the maximum steady-state radionuclide transfer rate into the water gap can be almost as great as if the container were not present.

In summary, we present here a framework for analyzing mass transfer of radionuclides through holes in partially-failed containers. Results illustrated for holes in thin-walled containers show that significant mass transfer can occur even if a small fraction of the container area is perforated. Extensions to the present work are planned, and experimental verification of the theories presented herein is invited.

2. Radionuclide Transport Through an Aperture in a Waste Form Container

P. L. Chambré

It is conjectured that waste form containers may fail due to chemical corrosion or due to mechanical effects. Subsequently, radionuclides may escape through the resulting apertures. The present analysis is concerned with their rate of escape from the impaired waste form.

The following assumptions are made. The transport of the specie from the opening into the surrounding space is by diffusion only. This space $\mathcal{R}$ consists of a water saturated medium, sufficiently fine grained compared with the aperture dimensions, to validate the diffusion mechanism into a continuum. The radionuclide in the waste form supplies a uniform concentration over an assumed time-invariant cross section of the aperture. The spatial extent of the concentration field away from the opening is small, as shown below, so that the canister wall can be treated as an infinite plane, see Fig. 1a.

2.1 The Model Equations

The governing equations for the radionuclide concentration $N(X,Y,Z,t)$ are

$$\frac{\partial N}{\partial t} = \frac{D_f}{K} \nabla^2 N - \lambda N, \text{ valid in } \mathcal{R},\ t > 0 \tag{1}$$

$$N = 0, \text{ valid in } \mathcal{R},\ t = 0 \tag{2}$$

$$V \frac{dN_w}{dt} = - D_f \epsilon_o \int_{S_a} \text{grad } N \, d\sigma - \lambda V N_w, \text{ valid on aperture surface } S_a,\ t \geq 0 \tag{3}$$

$$-D_f \ \epsilon_o \text{ grad } N = 0, \text{ valid on un-impaired canister surface, } t \geq 0 \tag{4}$$

N is a bounded function in $\mathcal{R}$, for $t > 0$.

D_f and K are the diffusion and retardation coefficients of the specie and λ its decay constant. ϵ_o is the porosity of the (water saturated) medium. N and N_w are the radionuclide concentrations in the half space and waste form respectively. V is the waste form volume.

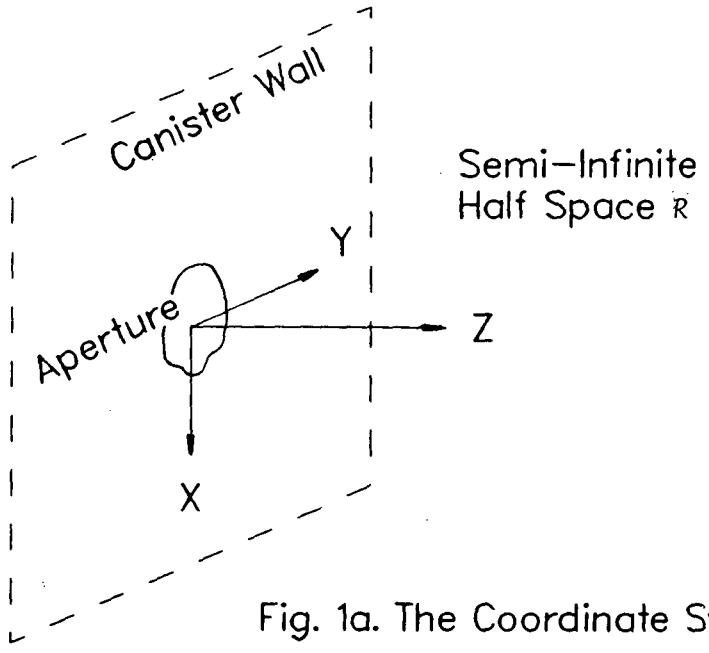

Fig. 1a. The Coordinate System

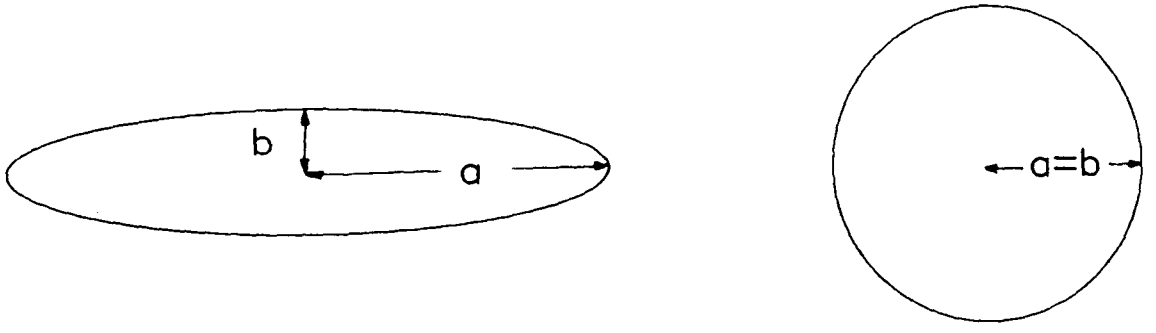

Fig. 1b. Aperture Shapes

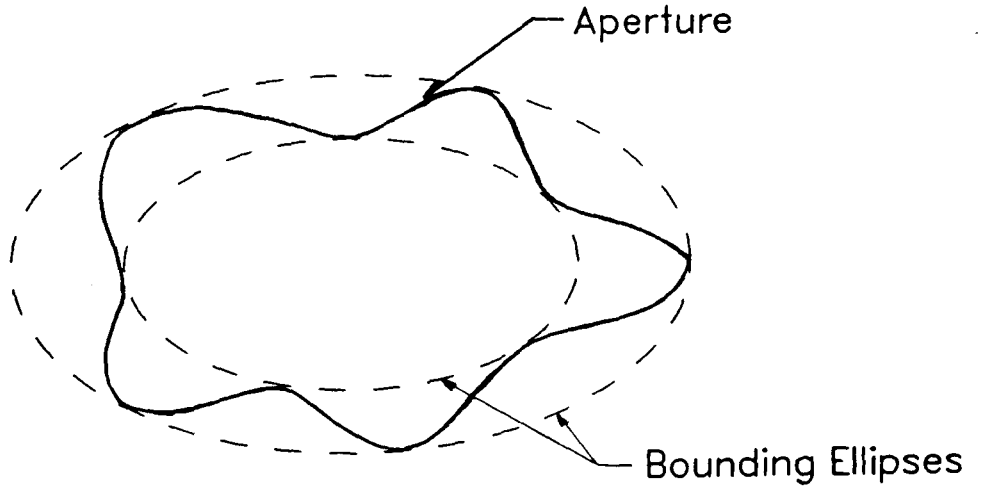

Fig. 1c. Bounding Contours

Equation (1) describes the specie balance due to diffusion, decay and storage in $\mathcal{R}$. Equation (2) states that, prior to the aperture opening, the specie concentration in $\mathcal{R}$ is zero. Equation (3) describes the rate of change of specie mass in the waste form due to diffusive mass transport through the opening and due to decay. It furnishes the specie concentration on the aperture surface S_a, since $N = N_w$ there. Equation (4) indicates the absence of diffusive mass transport through the impermeable part of the canister surface. The purpose of the following analysis is the determination of the time dependent mass flux through the aperture and the associated concentration field at steady state.

The analysis is simplified by the transformations

$$N(X,Y,Z,t) = e^{-\lambda t} n(X,Y,Z,t) \tag{5}$$

$$N_w(t) = e^{-\lambda t} n_w(t)$$

and the introduction of the following dimensionless variables

$$x = \frac{X}{a}\ ,\ y = \frac{Y}{a}\ ,\ z = \frac{Z}{a}\ ,\ A = \frac{S_a}{a^2}\ ,\ \theta = \frac{tD_f}{Ka^2}\ ,\ c(x,y,z,\theta) = \frac{n(X,Y,Z,t)}{n_w}\ ,\ c_w(\theta) = \frac{n_w(t)}{n_w} \tag{6}$$

Here a is a characteristic dimension of the aperture and n_w a reference concentration there. It is convenient to label the x,y coordinates separately from the z coordinate by writing

$$M = (x,y),\ c = c(M,z,\theta) \tag{7}$$

in the following.

The equations (1) - (4) transform to

$$\frac{\partial c}{\partial \theta} = \nabla^2 c,\ |M| < \infty,\ z > 0,\ \theta > 0 \tag{8}$$

$$c(M,z,0) = 0,\ |M| < \infty,\ z > 0 \tag{9}$$

$$\frac{dc_w}{d\theta} = -\beta \int_A \frac{\partial c(M,0,\theta)}{\partial z}\, d\sigma,\ M \epsilon A,\ \theta \geq 0 \tag{10}$$

$$\frac{\partial c(M,0,\theta)}{\partial z} = 0,\ M \notin A,\ \theta \geq 0 \tag{11}$$

where

$$\beta = \varepsilon_o K \frac{a^3}{V} \tag{10a}$$

and A is the dimensionless aperture surface. For the present it is assumed that the waste form volume is sufficiently large to make $\beta \simeq 0$, so that one can ignore the loss of specie through the opening during the time interval of interest. Then eq. (10) reduces to, with $c_w(0) = 1$,

$$c(M,0,\theta) = 1, \; M \epsilon A, \; \theta \geq 0. \tag{10b}$$

The case $\beta \neq 0$ is treated elsewhere.

2.2 The Transient Mass Flux

The solution of the equation system employs a Laplace transform with respect to the θ variable and yields for eq. (8), together with (9), for $\bar{c}(M,z,p)$

$$\nabla^2 \bar{c} - p\bar{c} = 0, \; |M| < \infty, \; z > 0. \tag{12}$$

The mixed boundary conditions (10b) and (11) transform to

$$\bar{c}(M,o,p) = \frac{1}{p}, \; M \epsilon A \tag{13}$$

$$\frac{\partial \bar{c}(M,o,p)}{\partial z} = 0, \; M \notin A \tag{14}$$

The Helmholtz equation (12) for the half space has the source function

$$H(M,M_o,p) = -\frac{1}{2\pi R} e^{-R\sqrt{p}} \tag{15}$$

where the source point M_o has the coordinates

$$M_o = (x_o, y_o) \tag{16}$$

and

$$\begin{aligned} R^2 &= (x-x_o)^2 + (y-y_o)^2 + z_o^2 \\ &\equiv r_{MM_o}^2 + z_o^2 \end{aligned} \tag{17}$$

The form of H assures a bounded solution for $\bar{c}$.

When equation (12) is treated formally as a Neumann problem, the solution is given by

$$\bar{c}(M,z,p) = \int_S H(M,M_o,p) \frac{\partial \bar{c}(M_o,o,p)}{\partial z} dM_o \tag{18}$$

where S is the entire surface of the waste form. On applying the boundary conditions (13) and (14) there results

$$-\frac{2\pi}{p} = \int_A \frac{e^{-r_{MM_o}\sqrt{p}}}{r_{MM_o}} \frac{\partial \bar{c}(M_o,o,p)}{\partial z} dM_o. \tag{19}$$

This represents a Fredholm integral equation of the first kind for the unknown (transformed) concentration gradient over the aperture surface A. The determination of the inverse transform of this gradient for (dimensionless) time θ is of interest. This corresponds to the asymptotic "small p" behavior of its transform. Hence expanding in powers of p

$$\frac{\partial \bar{c}(M,o,p)}{\partial z} = \frac{g_1(M,0)}{p} + \frac{g_2(M,o)}{p^{1/2}} + 0(1), \quad M\epsilon A. \tag{20}$$

The first term represents, on inversion, the steady state gradient on the aperture surface, which is obtained from the solution of equation (8) by having set $\frac{\partial c}{\partial \theta} = 0$. Its determination requires hence the solution of $c^S(M,z)$ of

$$\nabla^2 c^S = 0, \quad |M| < \infty, \quad z > 0 \tag{21}$$

$$c^S(M,o) = 1, \quad M\epsilon A \tag{22}$$

$$\frac{\partial c^S(M,o)}{\partial z} = 0, \quad M \notin A. \tag{23}$$

This problem will be treated in the next section and we consider for the moment

$$g_1(M,o) \equiv \frac{\partial c^S(M,o)}{\partial z}, \quad M\epsilon A \tag{24}$$

a known quantity. The second term in eq. (20) yields on inversion the asymptotic large time dependence of the aperture gradient. g_2 is found on substitution of eq. (20) into (19). Expanding the exponential function, one obtains on equating coefficients of power of p.

$$\int_A g_1(M_o,o)\ \frac{dM_o}{r_{MM_o}} + 2\pi = 0 \tag{25}$$

$$\int_A g_2(M_o,o)\ \frac{dM_o}{r_{MM_o}} + \int_A g_1(M_o,0)dM_o = 0.$$

This yields

$$g_2(M,o) = \left(-\frac{1}{2\pi}\int_A g_1(M_o,o)\ dM_o\right)\ g_1(M,o). \tag{26}$$

To obtain a measure of the total mass flux, one integrates the gradient over the opening. For this purpose we define the dimensionless shape factors

$$\bar{S}(p) = -\int_A \frac{\partial \bar{c}(M,o,p)}{\partial z}\ dM \tag{27a}$$

$$S_1 = -\int_A g_1(M,o)\ dM. \tag{27b}$$

Thus the integral of eq. (20) becomes with equations (26) and (27)

$$\bar{S}(p) = \frac{S_1}{p} + \frac{S_1^{\,2}}{2\pi p^{1/2}} + 0(1) \tag{28}$$

which yields on inversion the asymptotic representation

$$S(\theta) \sim S_1\left(1 + \frac{S_1}{(4\pi^3\theta)^{1/2}}\right),\ \theta \to \infty\ . \tag{29}$$

For early (dimensionless) time, the analytical behavior of the solution to eq. (19) is well known in that the leading term of the expansion of $\frac{\partial \bar{c}(M,o,p)}{\partial z}$ is constant over the aperture surface of area A yielding the following result for the shape factor

$$S(\theta) \sim \frac{A}{(\pi\theta)^{1/2}},\ \theta \to 0. \tag{30}$$

For some aperture configurations $S_1^{\,2} \simeq 2\pi A$. In that case the θ dependent contributions in equations (29) and (30) are identical and eq. (29) can be used as an approximation over the entire θ range. A circular opening for which $S_1 = 4$ (see Sec. 2.3), approximates this relationship with a 20% error.

This shape factor dependence on θ is shown in Fig. 2.

The practical use of the shape factor becomes apparent from the computation of the total aperture flux $\dot{m}(t)$ in terms of the original concentration variable N,

$$\dot{m}(t) = - D_f \varepsilon_o \int_{S_a} \frac{\partial N(X,Y,0,t)}{\partial Z} \, dXdY \, . \tag{31}$$

In view of equs. (5), (6) and the inverse of the transform of eq. (27a),

$$\dot{m}(t) = D_f \varepsilon_o (n_w e^{-\lambda t}) a S(t) \tag{32}$$

which is a general result, valid for an aperture of arbitrary shape. This yields the time dependence of the mass flux through the opening with help of eqns. (29) and (30).

Numerical estimates show that the time dependency is of lesser importance in the application to a repository setting where primarily the steady state solution is required. But the time dependent solution is of importance for the experimental validation of the theory.

2.3 The Steady State Mass Flux

As pointed out above, the determination of g_1 and thus S_1 requires the solution of the governing equations (21) - (23). At this point one must select a hole shape before a definitive solution is obtained. In absence of specific information about failure configurations, a family of elliptically shaped apertures has been selected whose eccentricity can be parametrically adjusted to approximate the range from very long slits to a circular hole, see Fig. 1b. What is essentially needed in equs. (29) and (32) is the shape factor S_1 as originally defined in eq. (27b), but we generalize the study beyond this immediate goal.

It is also of interest to determine the local gradient $g_1(M,o)$ over the aperture surface as well as the concentration field of a specie in the half space ($z > 0$). The solution to equs. (21) - (23) in ellipsoidal coordinates

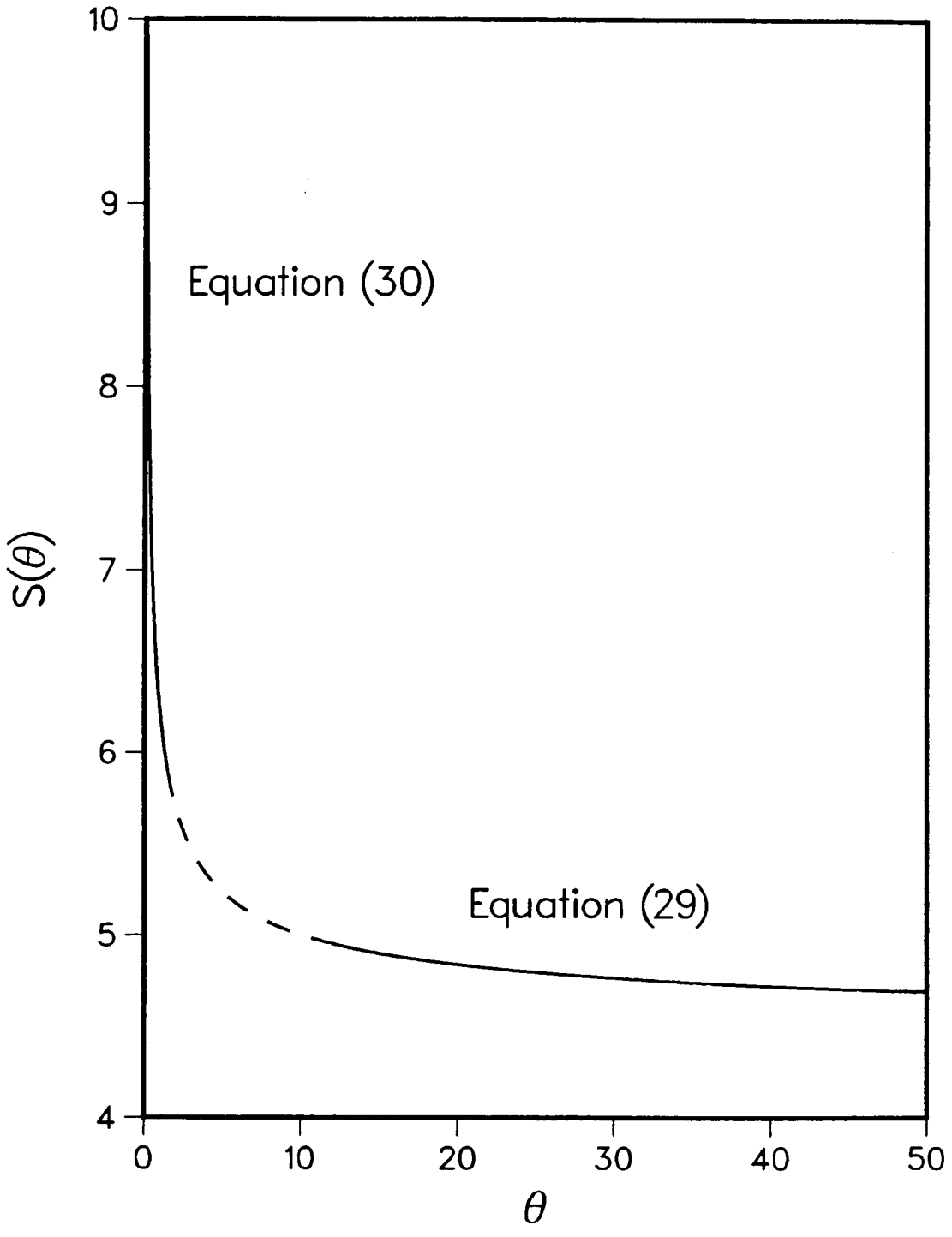

Fig. 2. The Time–Dependent Shape Factor

is given by

$$c^s(u) = \frac{F(u)}{F(0)} \quad , \quad 0 < u < \infty$$

with (33)

$$F(u) = \int_u^\infty \frac{du'}{\{(1+u')(\tilde{b}^2+u')u'\}^{1/2}}$$

where $\tilde{b} \simeq \frac{b}{a}$ is the dimensionless semi-axis of the ellipse and where the u coordinate describes the surface of the ellipsoid

$$\frac{x^2}{1+u} + \frac{y^2}{\tilde{b}^2+u} + \frac{z^2}{u} = 1. \tag{34}$$

Recall that the shape factor S_1 is a measure of the total mass flux through the aperture surface A. It can be evaluated by considering the concentration field at a very large distance from A, where the concentration field resembles that of a point source located at the origin of the half space, i.e.

$$c^s = \frac{S_1}{2\pi R}$$

with (35)

$$R^2 = x^2 + y^2 + z^2.$$

Thus as $u \to \infty$, $u \to R^2$ as seen from eq. (34), so that c^s becomes

$$c^s \simeq \frac{1}{F(0)} \int_{R^2}^\infty \frac{du'}{(u')^{3/2}} = \frac{2}{R} \frac{1}{F(0)} \quad , \quad R \to \infty. \tag{36}$$

Comparing this with eq. (35) yields the shape factor

$$S_1 = \frac{4\pi}{F(0)} \, . \tag{37}$$

A standard transformation reduces $F(0)$ to the tabulated elliptic integral of the first kind $K(m) = \int_0^{\pi/2} (1-m\sin^2\theta)^{-1/2} \, d\theta$,

$$F(0) = 2K\left(1 - \frac{b^2}{a^2}\right). \tag{38}$$

With this the shape factor for an elliptical opening is

$$S_1 = \frac{2\pi}{K\left(1 - \frac{b^2}{a^2}\right)} \tag{39}$$

Figure 3 shows the ratio of the shape factors of an elliptical to that of a circular aperture (for which $S_1 = 4$), their surface areas being equal, as a function of the eccentricity $\left(1 - \frac{b^2}{a^2}\right)$. This is computed from

$$\frac{S_1^{\text{ell.}}}{S_1^{\text{cir.}}} = \frac{\pi/2}{\sqrt{\frac{b}{a}}\, K\left(1 - \frac{b^2}{a^2}\right)}, \quad 0 < \frac{b}{a} \leq 1 \tag{40}$$

For small values of $\frac{b}{a}$, which models a long and narrow slit opening, one can use the asymptotic form of the elliptic integral

$$\frac{S_1^{\text{ell.}}}{S_1^{\text{cir.}}} = \frac{\pi/2}{\sqrt{\frac{b}{a}}\, \log\left(\frac{4}{b/a}\right)}, \quad \frac{b}{a} \ll 1. \tag{41}$$

The growth of this ratio, as $\frac{b}{a} \to 0$ is noteworthy.

For an irregularly shaped aperture, it is intuitively apparent that the total mass flux is bounded by the flux through inscribed and circumscribed elliptical apertures, see Fig. 1c. It follows rigorously that one can give upper and lower bounds for $S_1^{\text{irreg.}}$ by the corresponding inscribed and circumscribed shape factors.

$$S_1^{\text{inscr.}} \leq S_1^{\text{irreg.}} \leq S_1^{\text{circum.}} \tag{42}$$

Bounds which are calculated from eq. (39) become increasingly loose as the irregular shaped surface departs from their bounding elliptical shapes. Equation (42) is valid, however, for bounds other than those produced by elliptical configurations.

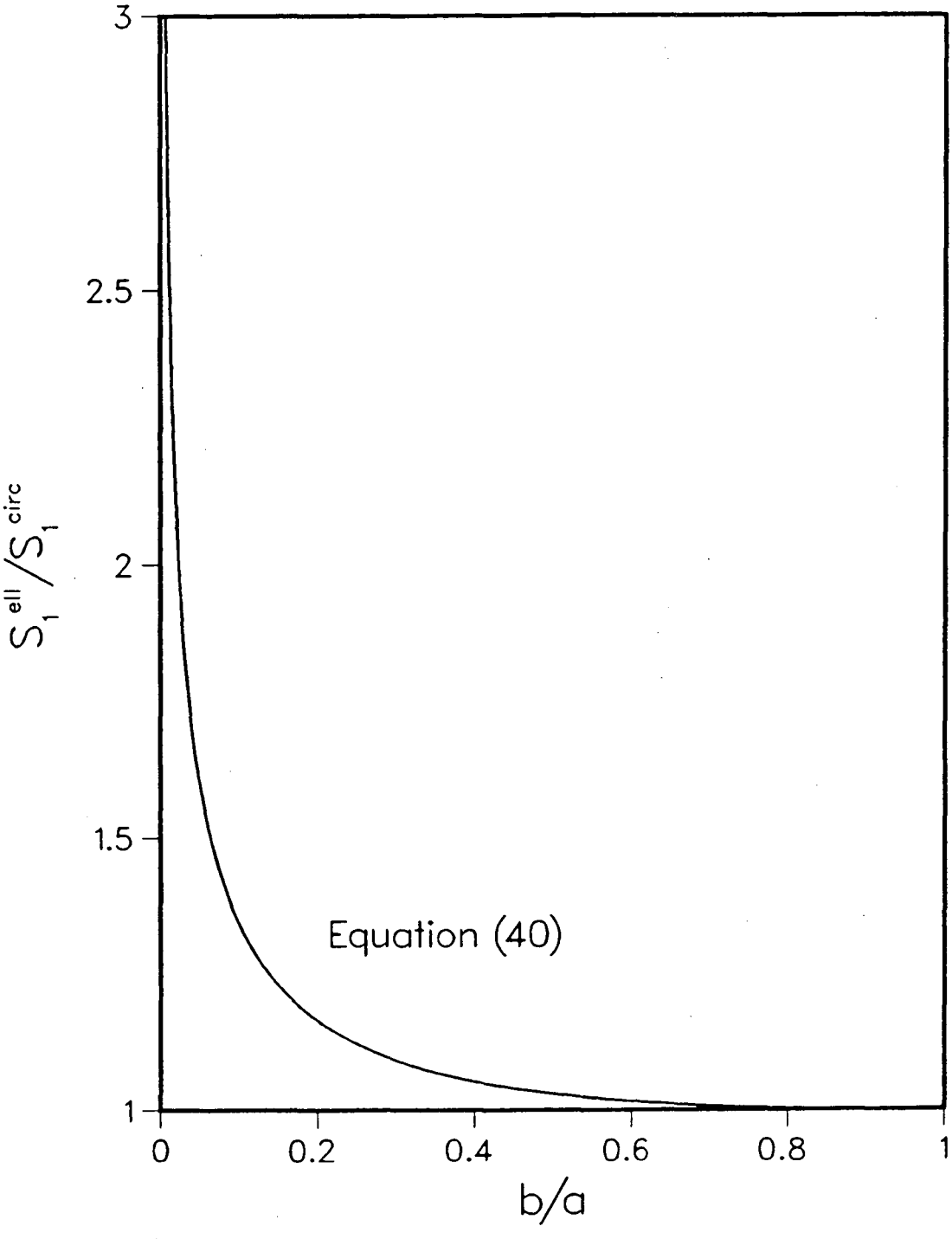

Fig. 3. The Steady State Shape Factor Ratio (Ellipse/Circle) as a Function of Semi–Axes Ratio

We consider next the local surface gradient at the aperture interface. It is computed from eq. (33) and yields

$$g_1(M,0) = -\frac{1}{\tilde{b}\sqrt{1-x^2-\frac{y^2}{\tilde{b}^2}}}\;\frac{1}{K(1-\tilde{b}^2)} \quad \text{(a)}$$

$$= -\frac{2/\pi}{\sqrt{1-r^2}} \quad \text{for } \tilde{b} = 1 \text{ and } r^2 = x^2 + y^2 \tag{43}$$

Comparison with eq. (34) shows that the magnitude of the local gradient at the aperture opening has a minimum at the center. It becomes infinite at the boundary of the hole, indicating a very pronounced increase in flux, which is shown in Fig. 4 for a circular aperture ($\tilde{b} = 1$).

Finally we consider the analysis of the nuclide's concentration field. The isopleths, in ellipsoidal coordinates, can be computed from the solution (33) in terms of an elliptic function. In the limiting case of a circular opening, for which $\tilde{b} = 1$, the solution takes the elementary form

$$c^s(u) = \frac{2}{\pi}\tan^{-1}\left(\frac{1}{\sqrt{u}}\right) \tag{44}$$

or transformed to cartesian coordinates with $r^2 = x^2 + y^2$

$$c^s(r,z) = \frac{2}{\pi}\sin^{-1}\left(\frac{2}{\sqrt{z^2+(1+r)^2}+\sqrt{z^2+(1-r)^2}}\right). \tag{45}$$

This result can be obtained by a number of other solution methods.*

The isopleths of (45) are shown in the following chapter. The decrease in concentration in the direction normal to the circular aperture is

$$c^s(0,z) = \frac{2}{\pi}\tan^{-1}\left(\frac{1}{z}\right) \tag{46}$$

by setting $x = y = 0$ in eq. (45). At a distance of ten aperture radii, c^s has fallen to approximately 5% of its orifice value. The decrease in

*After the completion of this report, Ref. (3) was brought to my attention in which eq. (45) is derived by an alternate method.

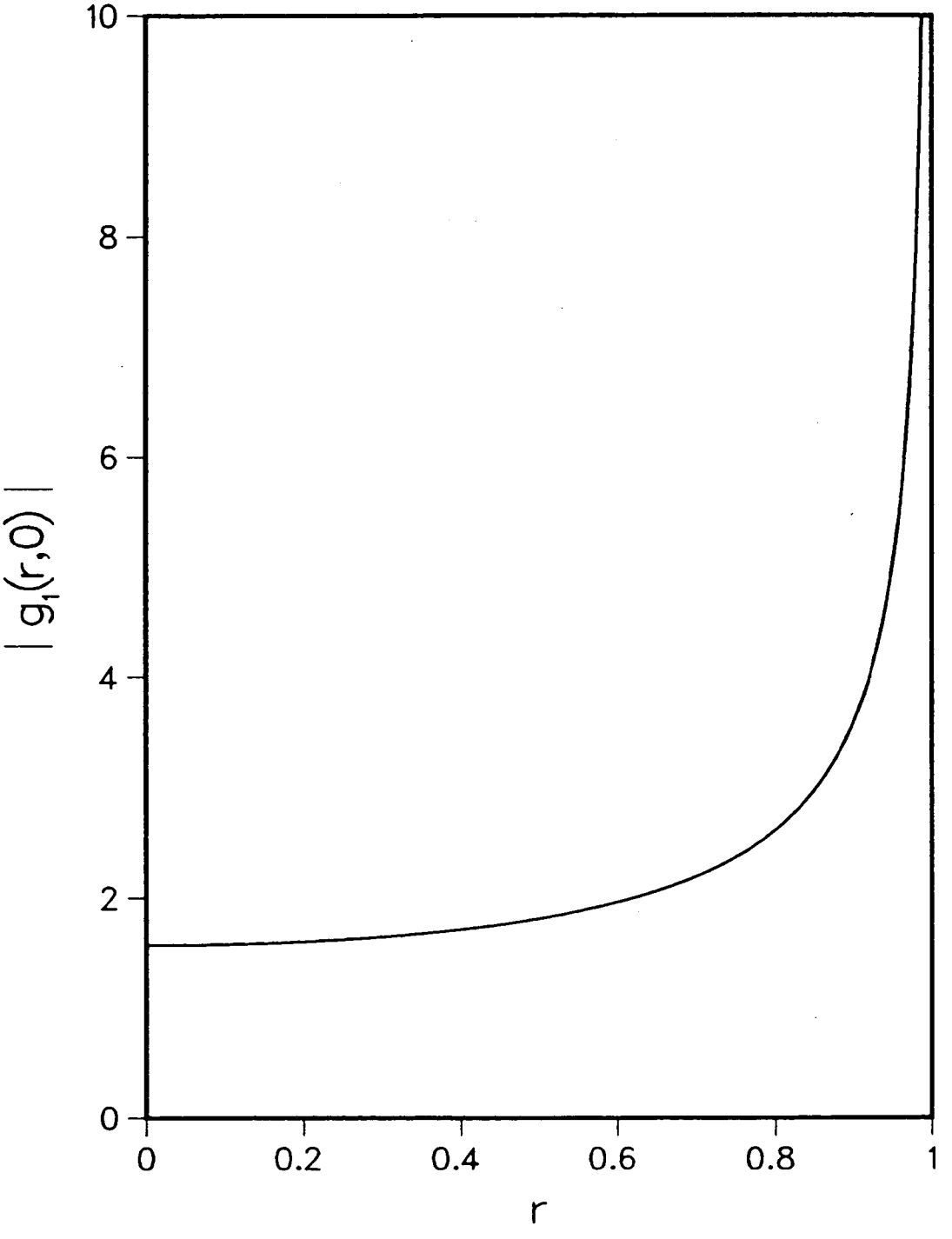

Fig. 4. The Magnitude of the Local Flux Function $g_1(r,0)$ for a Circular Aperture

concentration in the transverse direction is of comparable magnitude. Hence, if apertures are separated by a center to center spacing of ten radii, the total mass flux from such an assembly of holes can be obtained by superposition.

In the above, the case of an aperture in an infinitely thin container wall has been treated. For an approximate analysis of steady state diffusion through a wall of finite, dimensionless thickness $L = \left(\frac{w}{a}\right)$ one can proceed by a resistance analogue. Taking the reciprocal of the shape factor as a dimensionless resistance

$$\hat{R} = S^{-1} \tag{47}$$

the changes in concentration over parts of the circuit are presented as follows, see Fig. 5a,

$$(n_1 - n_{w_1}) = \frac{\dot{m}}{D_f a}\,\frac{\hat{R}_1}{\epsilon_1}\ , \quad (n_{w_1} - n_{w_2}) = \frac{\dot{m}}{D_f a}\,\hat{R}_3\ , \quad (n_{w_2} - n_2) = \frac{\dot{m}}{D_f a}\,\frac{\hat{R}_2}{\epsilon_2}\ . \tag{48}$$

ϵ_1, ϵ_2 are the porosities of the media adjacent to the wall.

Adding these equations yields

$$\dot{m} = D_f a\,(n_1 - n_2)\,\frac{1}{\hat{R}} = D_f a (n_1 - n_2) S \tag{49}$$

where

$$\hat{R} = \frac{\hat{R}_1}{\epsilon_1} + \frac{\hat{R}_2}{\epsilon_2} + \hat{R}_3$$

$$= \left(\frac{1}{S_1\epsilon_1} + \frac{1}{S_2\epsilon_2} + L\right) \tag{50}$$

in view of eq. (47) and the fact that the dimensionless resistance of the wall duct is equal to its dimensionless length. Hence the steady state shape factor for an aperture in a finite thickness wall is given by

$$S_{wall} = \left(\frac{1}{S_1\epsilon_1} + \frac{1}{S_2\epsilon_2} + L\right)^{-1}. \tag{51}$$

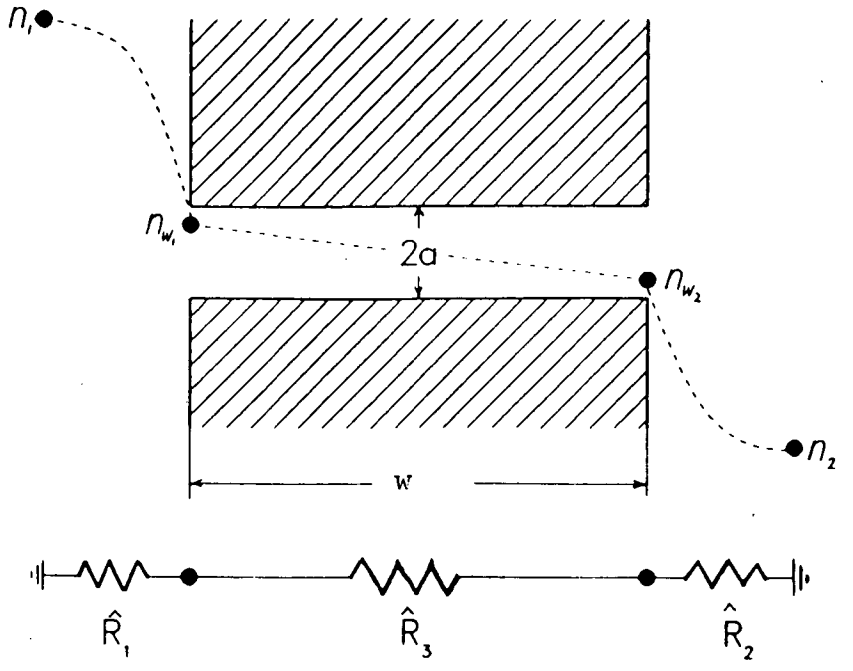

(5.a)

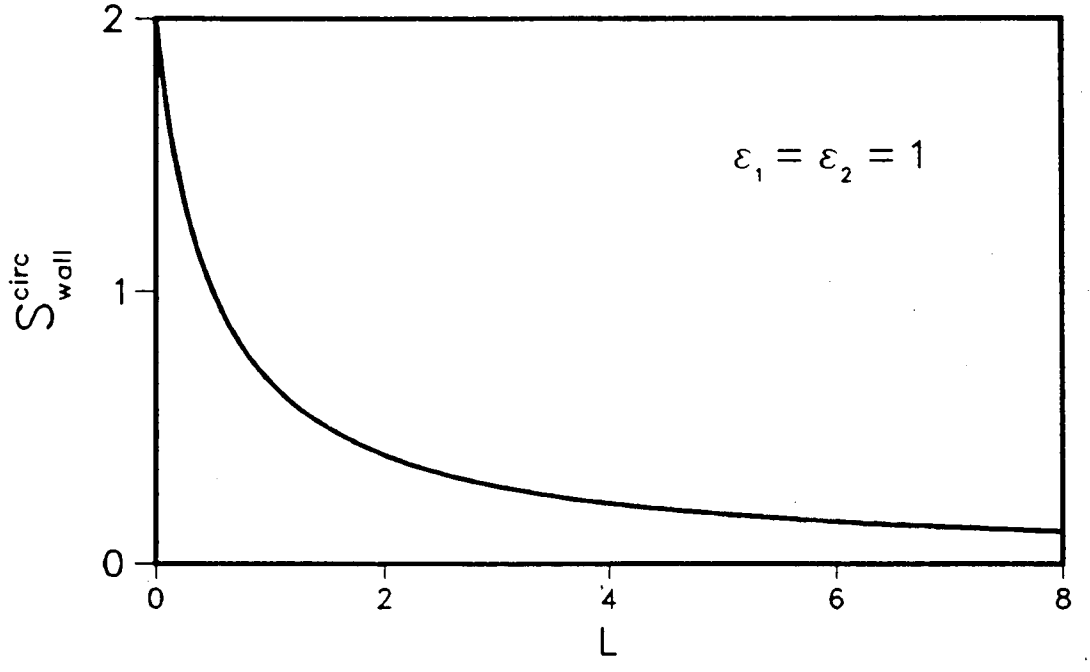

(5.b)

Figure 5. Analogue Circuit and Steady State Shape Factor for a Wall of Finite Thickness

The dependence on the thickness L and porosities $\epsilon_1 = \epsilon_2$ is noteworthy. For a circular aperture $S_1 = S_2 = 4$, so that

$$S_{wall}^{cir} = \frac{4}{\left(\frac{1}{\epsilon_1} + \frac{1}{\epsilon_2}\right) + 4L} \quad . \tag{52}$$

This is shown in Fig. 5b for ϵ_1 , $\epsilon_2 = 1$.

3. Numerical Illustrations

In this chapter we provide some numerical illustrations of the steady-state results obtained in Chapter 2.

3.1 Stable-Nuclide Diffusion From a Single Hole

In absence of decay, the steady-state dimensionless nuclide concentration field outside a waste container with a single circular hole is given by equation (45) of Chapter 2.

$$c^s(r,z) = \frac{2}{\pi} \sin^{-1} \left(\frac{2}{\sqrt{z^2 + (1+r)^2} + \sqrt{z^2 + (1-r)^2}} \right) \tag{45}$$

where z = normalized distance perpendicular to the hole surface

$r^2 = x^2 + y^2$, normalized distance along the hole

with **a** being the radius of the circular hole.

We can obtain the isopleths from equation (45)

$$r(c^s,z) = \sqrt{\frac{1-(z^2+1)\,\sin^2(\pi c^s/2) - \frac{1}{4} z^4 \sin^4(\pi c^s/2)}{\sin^2(\pi c^s/2) - \sin^4(\pi c^s/2)}} \quad , 0 \leq c^s \leq 1 \tag{53}$$

Using equation (53), the steady-state isopleth surfaces are shown in the domain $r>0$, $z>0$ in Figure 6.

At the position r=0 and z=0.5, the steady-state concentration is less than 70 per cent of the hole surface concentration, while at r=0 and z=12.7 the concentration has dropped to 5 per cent. All this can be calculated from equation (46). Also shown in dashed lines in Figure 6 are the diffusion paths, parallel to the concentration gradients. Near the edge of the hole the diffusive mass transfer is most intense.

3.2 Diffusion-Controlled Mass Release Rate Through a Hole

Using equation (43) the dimensional diffusive flux is

$$j(r,a) = - D_f \varepsilon_o n_w g_1(r,0)/a \tag{54}$$

$$= \frac{2D_f \varepsilon_o n_w}{\pi a \sqrt{1-r^2}} \quad , \; 0 < r \leq 1 \tag{55}$$

When the normalized distance along the hole is unity, the diffusive mass flux j(r, a) becomes infinite, consistent with the observation from Figure 6 that the diffusive mass transfer is most intense near the hole edge.

The steady-state dimensional mass release rate through a circular hole of radius **a** is

$$\dot{m}^s(a) = \int_o^a 2\pi r j(r,a) dr = 4 D_f \varepsilon_o \, a \, n_w \tag{56}$$

Therefore, the mass release rate through a hole increases linearly with the hole radius, magnitude of the diffusion

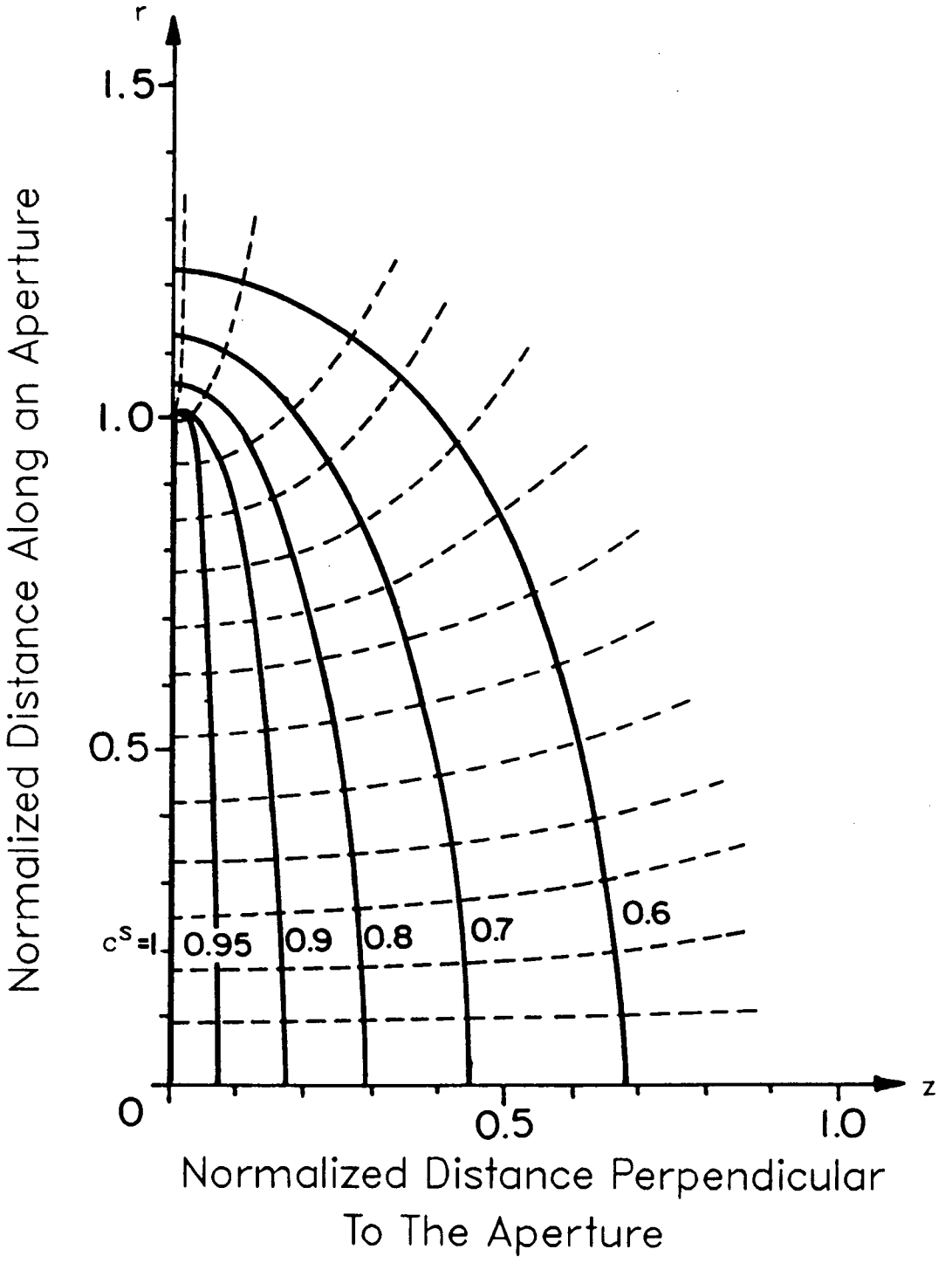

Figure 6. Surfaces of Non-dimensional Concentrations and Diffusional Paths Near an Aperture

coefficient, surface concentration, and porosity of the rock. This result is expected to be valid in porous media of small porosity, or for a hole size much larger than the grain size of the porous medium adjacent to the container.

3.3 Multiple Apertures on the Surface of a Cylindrical Waste Form

We now extend the results of the single, circular hole analysis to multiple apertures on a container. It is assumed that all apertures are of an identical size and shape.

Most nuclear waste containers, such as spent fuel rods or reprocessed waste containers, are expected to be cylindrical. If multiple apertures are present on such a cylinder, and if one seeks to predict the total mass transfer rate from all holes, the total mass transfer rate is the sum of contributions from all holes. For this sum to be obtained from the single-hole equations, one must first determine if the concentration fields from adjacent holes overlap, causing the concentration fields to interfere with the prescribed concentration boundary condition at the aperture. In other words, how far must the holes be separated for the summation to be valid? From eq. (45), it is seen that at $z=0$, $r=10$, then $c^S=0.064$, and the concentration has fallen to negligible levels about 10 hole radii away, so that the summation rule might apply. For example, on a

cylindrical container, with a radius of 0.15 m and a length of 2.46 m, there can be 235 identical 1-cm radius holes, 23,000 0.1-cm holes, or 94,000 0.05-cm holes for this summation rule to be valid.

3.4 Release Rate from Multiple Apertures in a Container in Contact with Porous Medium

For holes sufficiently separated as described in Section 3.3, the total mass transfer rate through ν holes of radius **a** would be

$$\dot{m}_t^s(\nu, a) = \nu \dot{m}^s(a) \tag{57}$$

Or from equation (56),

$$\dot{m}_t^s(\nu, a) = 4\nu D_f \varepsilon_o a N_w \tag{58}$$

It may be instructive to compare the total rate of release from ν holes on a container to the release rate from a bare cylinder of the waste form, both subject to diffusion only. The steady-state diffusive mass transfer rate from a waste form cylinder of radius f_1 and length ℓ in contact with porous rock is given by equation (7.5.2) of Chambre' **et al.**[2],

$$\dot{m}_c^s(f_1, \ell) = 2\pi D_f \varepsilon_o N_w \ell / \log(\ell / f_1) \tag{59}$$

where the end effects have been neglected.

To compare the two release rates for fixed waste-cylinder dimensions, define the following dimensionless mass transfer ratio:

$$\alpha(\nu, a) = \dot{m}_t^s(\nu, a)/\dot{m}_c^s(f_1, \ell) \tag{60}$$

The dimensionless mass transfer ratio is the total rate of mass transfer from apertures of radius **a** to the total mass transfer rate from a cylinder with no cladding. Using equations (58) and (59) one can rewrite equation (60) in the following form:

$$\alpha(\nu, a) = \frac{2a\nu}{\pi\ell} \log(\ell/f_1) \tag{61}$$

In Figure 7, $\alpha(\nu, a)$ is plotted as a function of ν for aperture radii of a=1 cm, 1 mm, and 0.5 mm, located on the surface of a waste form with f_1= 0.15 m, ℓ=2.46 m. Ratios of the total hole area to the total cylindrical surface (including holes), but excluding end surfaces, are indicated on each of the three lines of $\alpha(\nu, a)$. Figure 7 shows that the radionuclide transfer rate from a waste container with numerous small holes can actually exceed that from a bare waste cylinder of the same dimensions. On a bare waste form cylinder, the mass transfer rate would be uniform over the surface of the cylinder, but in a cylinder with numerous holes, the gradient at all hole edges is

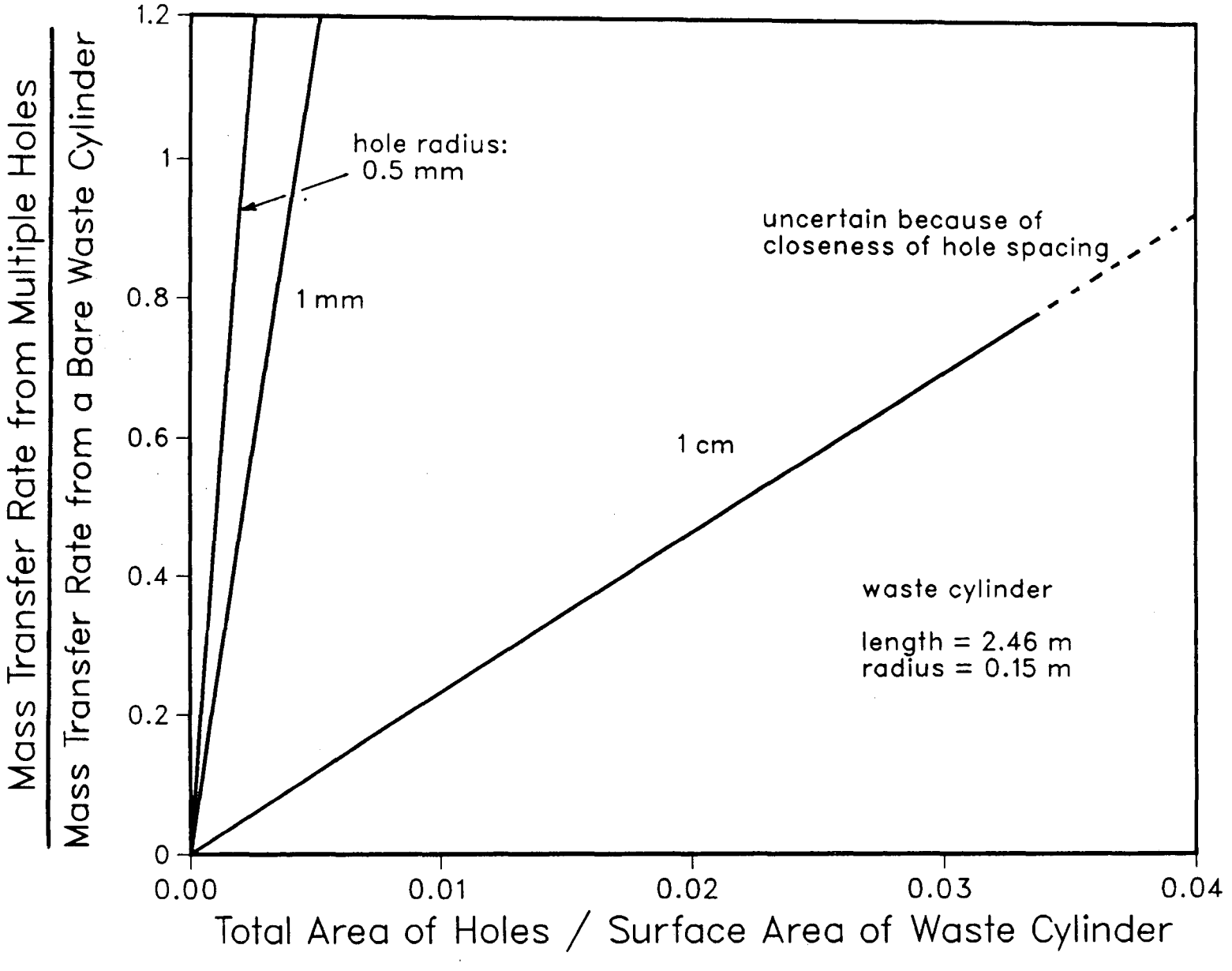

Figure 7. Radionuclide Transfer Rate from Multiple Apertures and a Bare Waste Cylinder

infinite, leading to more intense mass transfer. For waste cylinder of f_1=0.15 m and ℓ = 2.46 m, the mass transfer ratio of eq. (61) can be written as

$$\alpha(\nu,a) = 3.13 \times 10^{-3} \nu a \qquad (62)$$

If all holes are 1 mm and there are 3,200 holes, then $\alpha > 1$, and the mass transfer rate from a waste cylinder with holes exceeds that from a bare waste cylinder of equivalent dimensions. As the number of holes increase and the holes become closely spaced, the concentration fields from adjacent holes begin to overlap appreciably, and the superposition of single-hole solutions is no longer valid. This occurs at an area ratio of about 0.033 for holes of 1 cm radius.

3.5 Effect of a Water Gap Between Container and Porous Medium

A water gap between the perforated container and the porous medium, as shown in Figure 8, can result in release rates different from those estimated in Section 3.4. To illustrate, we develop a simplified analysis by assuming no convection in the water gap.

The calculations of Section 3.3 for a perforated container in contact with an infinite porous medium also apply to a container in contact with infinite water, of unit porosity, if convection is negligible and transport is entirely by diffusion.

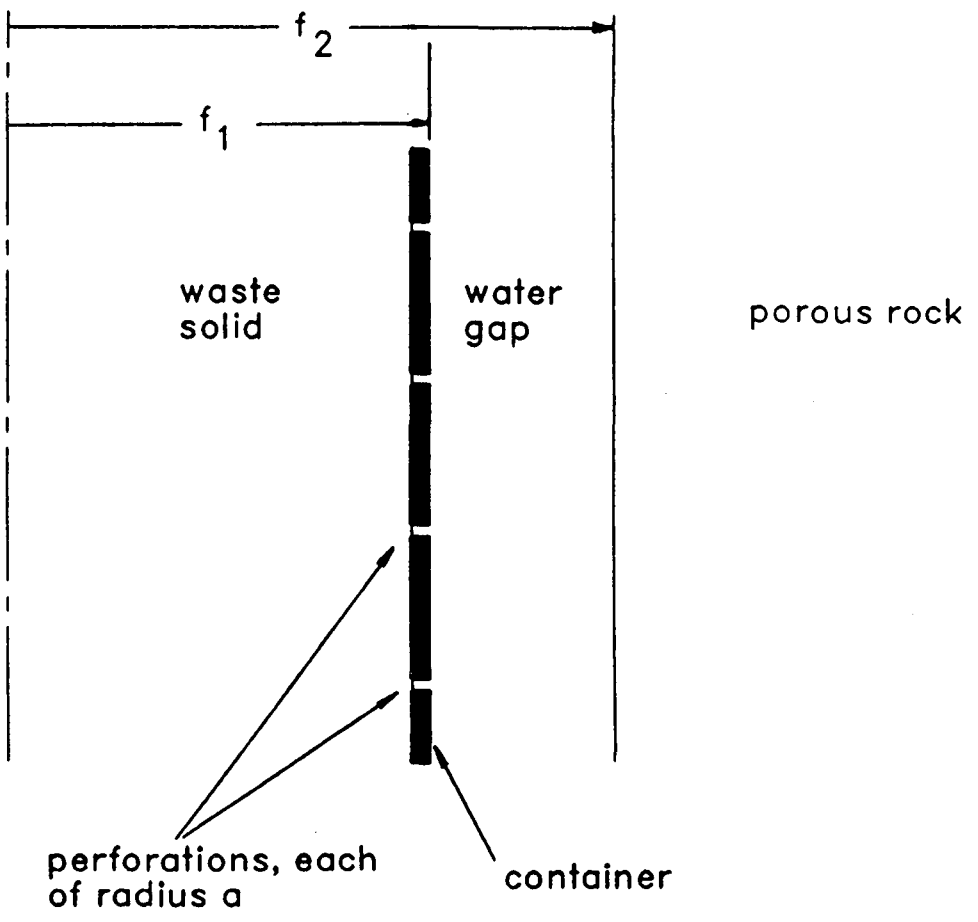

Figure 8. Geometry For a Water Gap Between Container and Porous Rock

The analytical solutions of Section 2.3 for steady state assumed zero concentration in water at an infinite distance in the Z direction from the container. If there is a finite far-field concentration N_∞ in ground water far from the waste, the analytical solutions can be used by redefining $c^s(r,z)$ and rewriting equation (45) as:

$$c^s(r,z) = \frac{N(r,z) - N_\infty}{N_w - N_\infty} = \frac{2}{\pi} \sin^{-1} \frac{2}{\sqrt{z^2 + (1+r)^2} + \sqrt{z^2 + (1-r)^2}} \qquad (63)$$

and equation (58) for the mass transfer rate $\dot{m}_t^s$ through ν apertures in a container surrounded by water, with no convection, becomes:

$$\dot{m}_t^s = 4\nu D_f a (N_w - N_\infty) \qquad (64)$$

From equation (63) we find that at reduced distances z = 10 and 100 the concentration differences are:

$$(N(0,z) - N_\infty) / (N_w - N_\infty) = 0.064 \quad , \quad \text{for } z = 10$$
$$= 0.0064 \quad , \quad \text{for } z = 100$$

Thus, to a good approximation, for a container with 1-mm holes a few centimeters or more of water are sufficient for the water to appear to the holes as an infinite diffusing medium.

From equation (63) it can be demonstrated that at a distance z from the container equal to or greater than ten hole radii, the concentration in the water is essentially constant over a plane normal to Z. Therefore, we expect that if the porous medium is

positioned ten hole radii or more from the container it will be exposed to a concentration that is essentially uniform over its surface.

For these reasons, we will use equation (64), derived for an infinite diffusing medium, as an approximation for the water gap of finite thickness, and we will adopt the concentration N_r at the porous-medium interface as the concentration N_∞ in equation (64). There results:

$$\dot{m}_t^s = 4\nu\, D_f\, a\, (N_w - N_r) \tag{65}$$

The steady-state mass-transfer rate $\dot{m}_t^s$ is also given by applying equation (59), but with N_r as the concentration and f_1 as the radius at the inner surface of the medium of porosity ε_0:

$$\dot{m}_t^s = 2\pi D_f\, \varepsilon_0 N_r \ell \,/\, \log(\ell / f_1) \tag{66}$$

Combining equations (65) and (66) to eliminate N_r, we obtain

$$\dot{m}_t^s = \frac{2\pi\, D_f\, \varepsilon_0 N_w\, \ell}{\log(\ell/f_1) + \dfrac{\pi\varepsilon_0 \ell}{2\nu\, a}} \tag{67}$$

Now, we seek an expression for the steady-state release through the water gap and porous medium if the waste container is not present. Because of the low diffusional resistance of a few centimeters of water continuum as compared with that of the

surrounding low-porosity rock, we expect that the steady-state concentration N_r will be close to the concentration N_w at the waste surface. Assuming $N_r = N_w$ for no container, the steady-state mass-transfer rate is:

$$\dot{m}_t^s = 2\pi D_f \varepsilon_0 N_w \ell \; / \; \log(\ell / f_1) \tag{68}$$

The ratio $\alpha(\nu, a)$ of the mass-transfer rates with and without a perforated container is then:

$$\alpha(\nu,a) = \frac{1}{1 + \dfrac{\pi\varepsilon_0 \ell}{2\nu\, a \log(\ell/f_1)}} \tag{69}$$

The results are plotted in Figure 9, using the same parameter values as in Figure 7 of Section 3.4, with a 10-cm water gap. Similar to the results in Figure 7, a small fraction of the container area exposed by small holes, e.g., a = 1 mm or less, results in steady-state release rates that are almost as great as if the container were not present. Within the framework of the assumptions stated herein for the water-gap analysis, the maximum mass-transfer rate through a container with holes is no greater than the mass-transfer rate with no container. We expect that convective mixing in the water gap will steepen the curves in Figure 9 and bring the mass-tranfer rate with holes even nearer the mass-transfer rate with no container.

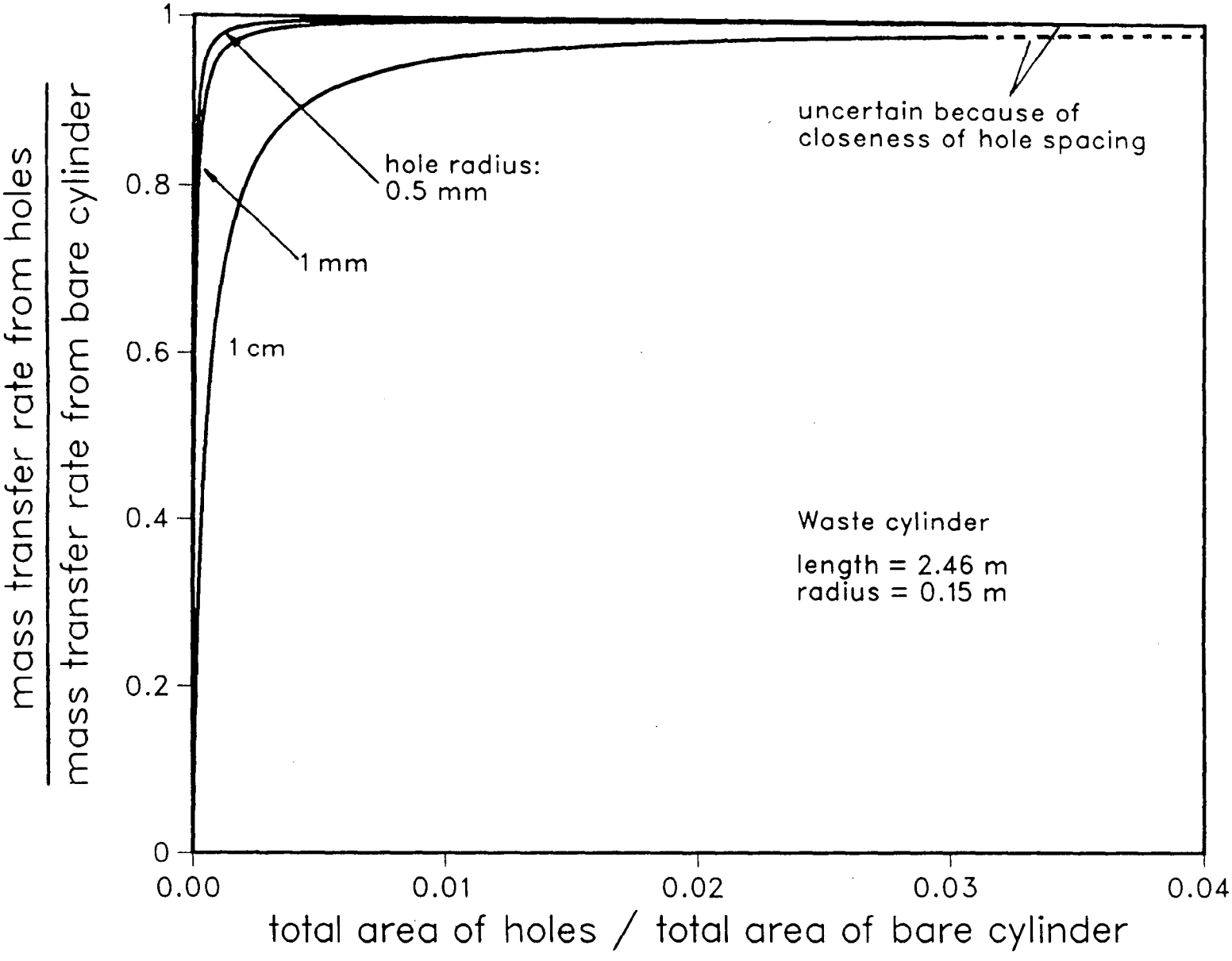

Figure 9. Radionuclide Transfer Rates from Multiple Holes Facing a Water Gap and from a Bare Waste Cylinder

4. Conclusions

In Chapter 3 are numerical illustrations of some of the analytical results derived in Chapter 2. These calculations show that radionuclide transfer from multiple apertures can be significant and may approach or even exceed the mass transfer rate calculated for bare waste forms.

There are several possible implications for the repository program.

1. The U. S. Nuclear Regulatory Commission has not elaborated on the meaning of "substantially complete containment". This study indicates that radionuclide transfer rates can be significant from partially-failed waste containers, such as spent-fuel cladding. Diffusion through small apertures and cracks in the container can affect compliance with substantially complete containment.

2. Spent-fuel cladding may not be an effective barrier if many small perforations are anticipated.

3. Although partially-failed containers and container-corrosion products may present an important long-term barrier to

release of radionuclides, small through holes have the potential of bypassing the effectiveness of these barriers.

4. To take credit for the long-term effectiveness of partially-failed containers as barriers to radionuclide release, details on the number and size of small penetrations and their growth with time will be needed.

5. For thin-walled containers with a sufficient number of small perforations, waste performance can be estimated by assuming waste form in direct contact with surrounding backfill or porous rock.

For the illustrations presented in Chapter 3 it is conservatively assumed that the holes are in a container of negligible thickness. The analytical solutions of Chapter 2 also show the effect of finite container wall thickness. Numerical illustrations for finite-thickness containers and for other hole shapes will be presented in a future report.

The analytical solutions of Chapter 2 can be--and should be--verified by simple laboratory experiments.

5. Nonmenclature

Symbol	Variable	Dimension
Basic Variables		
a	Characteristic dimension of aperture	[L]
b	Characteristic dimension of aperture	[L]
c^s	Steady-state radionuclide concentration	
D_f	Diffusion coefficient	$[L^2/T]$
f_1	Radius of waste cylinder	[L]
g_1, g_2	Local surface gradient	
j	Radionuclide flux	$[M/L^2\text{-}T]$
K	Retardation coefficient	
ℓ	Length of waste cylinder	[L]
$\dot{m}$	Radionuclide transfer rate	[M/T]
M_0	Source point	
N	Radionuclide concentration	$[M/L^3]$
N_r	Radionuclide concentration at water-gap/rock interface	$[M/L^3]$
N_w	Radionuclide concentration in the waste form	$[M/L^3]$
N_∞	Radionuclide concentration at infinity	$[M/L^3]$
R	Space domain	
$\hat{R}$	Mass transfer resistances	
S	Waste form surface area	$[L^2]$
S_a	Surface area of the aperture	$[L^2]$
S_1, $\bar{S}$	Shape factors	
t	Time	[T]

u	Ellipsoidal coordinate	[L]
V	Volume of the waste form	[L^3]
w	Thickness of the container	[L]
X,Y,Z	Space coordinates	[L]
α	Mass flux ratio	
ε_0	Porosity	
λ	Decay constant	[T^{-1}]
ν	Number of holes	

Transformed Variables

A	$= S_a/a^2$
c	$= n \,/\, n_w$
$c_w(\theta)$	$= n_w(t) \,/\, n_w$
L	$= w/a$
M	$= (x,y)$
n	$= N \,/\, \exp(-\lambda t)$
$n_w(t)$	$= N_w(t) \,/\, \exp(-\lambda t)$
R^2	$= x^2 + y^2 + z^2$
r^2	$= x^2 + y^2$
x	$= X \,/\, a$
y	$= Y \,/\, a$
z	$= Z \,/\, a$
β	$= \varepsilon_0 K a^3 \,/\, V$
θ	$= tD_f \,/\, Ka^2$

6. References

1. U. S. Nuclear Regulatory Commission, "Disposal of High-Level Radioactive Wastes in Geologic Repositories", Title 10, Code of Federal Regulation, Part 60, 1983.

2. Chambre', P. L., Pigford, T. H., Sato, Y., Fujita, A., Lung, H., Zavoshy, S., Kobayashi, R. "Analytical Performance Models", LBL-14842, 1982.

3. Rae, J., "Leaks from Circular Holes in Intermediate-Level Waste Canisters", AERE-R.11631, 1985.

LAWRENCE BERKELEY LABORATORY
TECHNICAL INFORMATION DEPARTMENT
UNIVERSITY OF CALIFORNIA
BERKELEY, CALIFORNIA 94720